Cooperative Energy Transfer Controls the Spontaneous Emission Rate Beyond Field Enhancement Limits

Mohamed ElKabbash, Ermanno Miele, Ahmad K. Fumani, Michael S. Wolf, Angelo Bozzola, Elisha Haber, Tigran V. Shahbazyan, Jesse Berezovsky, Francesco De Angelis, and Giuseppe Strangi

Phys. Rev. Lett. **122**, 203901 — Published 22 May 2019

DOI: 10.1103/PhysRevLett.122.203901

Cooperative Energy Transfer Controls the Spontaneous Emission Rate Beyond Field Enhancement Limits

Mohamed ElKabbash[1*], Ermanno Miele[1, 2], Ahmad K. Fumani[1], Michael S. Wolf[1], Angelo Bozzola[2], Elisha Haber[1], Tigran V. Shahbazyan[3], Jesse Berezovsky[1], Francesco De Angelis[2], Giuseppe Strangi[1,2,4*].

[1.] Department of Physics, Case Western Reserve University, 10600 Euclid Avenue, Cleveland, Ohio 44106, USA.

[2.] IIT - Istituto Italiano di Tecnologia, via Morego 30, 16163 Genova, Italy.

[3.] Department of Physics, Jackson State University, Jackson, Mississippi 39217, USA.

[4.] CNR-NANOTEC, Istituto di Nanotecnologia and Department of Physics, University of Calabria, Italy.

*Correspondence authors E-mail: mke23@case.edu, gxs284@case.edu.

Quantum emitters located in proximity to a metal nanostructure individually transfer their energy via near-field excitation of surface plasmons. The energy transfer process increases the spontaneous emission (SE) rate due to plasmon-enhanced local field. Here, we demonstrate significant acceleration of quantum emitter SE rate in a plasmonic nano-cavity due to cooperative energy transfer (CET) from plasmon-correlated emitters. Using an integrated plasmonic nano-cavity, we realize up to six-fold enhancement in the emission rate of emitters coupled to the same nano-cavity on top of the plasmonic enhancement of the local density of states. The radiated power spectrum retains the plasmon resonance central frequency and line-shape, with the peak amplitude proportional to the number of excited emitters indicating that the observed cooperative SE is distinct from super-radiance. Plasmon-assisted CET offers unprecedented control over the SE rate and allows

to dynamically control the spontaneous emission rate at room temperature which can enable SE rate based optical modulators.

Ordinary fluorescence arises from the decay of excited quantum emitters (QEs) to lower energy states by SE where QEs interact independently with the radiation field. This interaction can be controlled by modifying the emitter's electromagnetic environment. The SE rate is directly proportional to the electromagnetic local density of states (LDOS) [1-3], i.e., the number of electromagnetic modes available for the emitter to radiate into per unit volume and frequency interval. LDOS can be modified by, e.g., placing an emitter inside a cavity. Cavity enhanced SE rate is proportional to the ratio of cavity quality factor Q to modal volume *V,* known as the Purcell effect [3] . The emitters' SE rate has been significantly enhanced using plasmonic nanocavities (PNCs) supporting localized surface plasmon (LSP) modes [2-5]. The LDOS enhancement in a PNC results from strong field confinement within small plasmon mode volume, so a QE transfers its energy to a resonant plasmon mode with an energy transfer rate Γ^{ET} faster than the free-space SE rate (**Fig. 1a**). Subsequently, a PNC acts as an optical antenna radiating transferred energy with a significantly faster rate due to its large size and dipole moment [2,6]. Accordingly, following the excitation of a QE, the emission rate is proportional to Γ^{ET}. However, the SE rate of an individual QE is restricted by ultimate limits on plasmonic field enhancement [7,8].

When an ensemble of QEs is coupled to a plasmonic structure, SE can be greatly accelerated by cooperative effects arising from plasmon-assisted correlations between QEs. For example, interactions of QE with common radiation field enhanced by resonant Mie scattering are predicted to lead to plasmon-enhanced super-radiance characterized by SE rate proportional to the *full ensemble size* including both excited and ground-state QEs[9-13]. However, the

plasmonic enhancement of radiation coupling is offset by relatively strong absorption, compared to scattering, in small metal structures [10] , which inhibits coherence buildup that precedes super-radiance burst from incoherently excited emitters [14,15]. An observation of plasmon-enhanced super-radiance, accordingly, remains challenging [16].

Conversely, strong plasmon absorption may lead to another cooperative effect in a system of *N* excited QEs coupled to a plasmonic resonator that does *not* require coherence buildup between excited QEs [17,18]. If plasmon frequency is tuned to resonance with QEs emission frequency, the indirect plasmonic coupling between QEs gives rise to collective states that transfer their energy to a plasmon *cooperatively* at a rate $\Gamma_c^{ET} = \sum_i^N \Gamma_i^{ET}$ where Γ_i^{ET} is the energy transfer rate of individual QEs (**Fig. 1b**). Note that the Förster resonance energy transfer rate from QEs to a plasmon is determined by the spectral overlap between the donor (QE) emission band and the acceptor (plasmon) absorption band [19]**.** Since the plasmon spectral band is broader than that of QEs, the cooperative energy transfer (CET) rate is relatively insensitive, in contrast to super-radiance [20,21], to natural variations of QEs emission frequencies, e.g., due to direct dipole coupling. Following CET to a plasmon mode, the possible energy flow pathways include (i) energy transfer from PNC to QEs, (ii) energy dissipation within PNC through Ohmic losses, and (iii) PNC antenna radiation. If the antenna's radiation efficiency is high, while the overlap between QEs' emission and absorption bands is relatively weak, the energy is mainly radiated away at approximately rate Γ_c^{ET}. Note that the values of individual rates Γ_i^{ET} are determined by the plasmon LDOS at the QEs' positions and can vary significantly depending on the system geometry [18,19]. However, if the LDOS does not change significantly in the region where QEs are distributed, Γ_i^{ET} are all comparable and the cooperative rate Γ_c^{ET} scales *linearly with the*

67 *number of excited emitters (N), hence the excitation power*. Accordingly, the ensemble SE
68 mediated by CET to plasmonic antenna can be controlled directly by the excitation power.

69 Here, we report the experimental observation of a cooperative SE from an ensemble of *N* excited
70 QEs resonantly coupled to a PNC acting as a plasmonic antenna. We observe up to six-fold
71 increase of the ensemble SE rate relative to the plasmonic LDOS enhancement which is linear in
72 the excitation power. Simultaneously, the measured photoluminescence spectrum retains the
73 plasmon resonance lineshape while the overall emission intensity increases linearly with the
74 excitation power. These observations imply that the radiation is emitted by the plasmonic
75 antenna following CET from excited QEs[17]. The linear dependence of the ensemble SE rate on
76 the number of excited QEs (as opposed to total number of emitters [21-23]) has not been
77 observed previously. Such dependence as well as the incoherent nature of CET
78 mechanism[17,18] that does not require coherence buildup [14,15] , in contrast to super-
79 radiance, provides a unique possibility for dynamically controlling the SE rate in the *same*
80 electromagnetic environment by varying excitation power (*Supplementary Note* **2.1**) . We
81 experimentally exploit CET to dynamically control SE rate by modulating the excitation power,
82 resulting in *reversible* increase and decrease of the SE rate at room temperature, which was only
83 possible in previous works using complex photonic devices at cryogenic temperatures [24,25].
84 The cooperative enhancement of the ensemble SE rate takes place on top of the plasmon LDOS
85 enhancement for individual emitter's SE rate paving the way towards SE rate control beyond
86 field enhancement limits [7,8]. This is important for short-distance optical communication, to
87 increase the modulation rate [6], and for optical data storage [26].

88

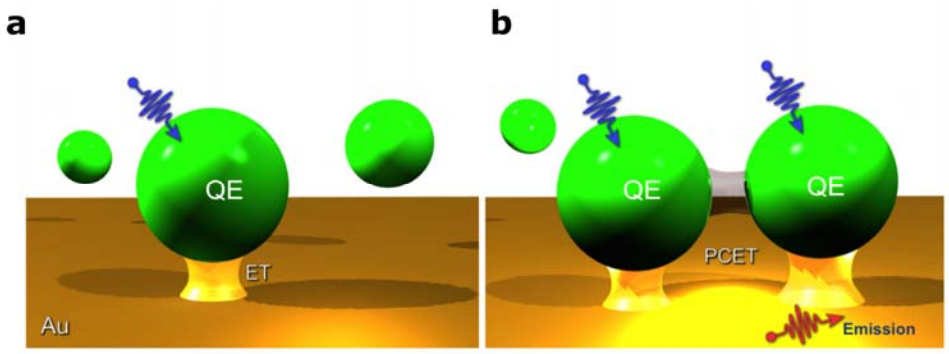

Figure 1| **(a)** An excited QE coupled to plasmonic resonator non-radiatively transfers its energy, at a rate to the plasmon mode, which radiates it away. **(b)** An ensemble of QEs coupled to a resonant plasmon mode transfer their energy to it cooperatively at a rate that is the sum of individual rates[18].

To demonstrate the effect, we fabricated three dimensional hollow PNC [27,28] (*Supplementary methods* [29]). **Fig. 2a** and **Fi**g. **2b** show SEM image of PNC array, and single PNC cross-section, respectively. The PNCs are composed of a cylindrical polymeric scaffold, 20 nm thick and 450 nm height, on which a 20nm gold layer was conformally deposited. The geometry of the PNCs was chosen to ensure strong radiation directionality (*Supplementary information,* **Fig. S2**). The radiation pattern from our PNC is highly directional and the large size of the PNC increases the antenna radiative efficiency [4,6,30] to ensure that the major energy pathway following energy transfer process is antenna radiation and that the collected photons are from antenna radiation. CdSe/ZnS quantum dots (QDs) were spin-coated on the polymeric scaffold onto which the plasmonic shell is formed (**Fig. 2c** and **2d**). We chose QDs as our QEs over, e.g., fluorophores, as they have larger dipole moments which increases non-radiative energy transfer efficiency [5], and exhibit relatively weak absorption in the photoluminescence frequency range to reduce reabsorption which is important to demonstrate CET (*Supplementary information*, **Fig. S3**). The integrated PNC is designed such that QEs are at approximately the same distance away from the plasmonic shell to excite LSPs with the same energy transfer rate, i.e., (**Fig. 2d**). This relation is robust even for large fluctuations in QEs positions since the LSP

electric field inside PNC is nearly uniform. The PNC measured (**Fig. 2e)** and calculated (**Fig. 2f**) LSP resonance are in close agreement. To control for frivolous QD-metal interactions, we prepared a reference sample where the QDs were spin-coated on an Au film. **Fig. 2g** compares the QDs photoluminescence collected from a single PNC and from the reference sample with excitation wavelength and intensity 18.5 W/cm^2. The photoluminescence maximum is blue shifted from 638 nm (reference) to 631nm (PNC) towards the LSP resonance peak (~628nm) [31]. The blue-shift in the photoluminescence maximum and the high directionality and radiative efficiency of our PNC ensure that collected photoluminescence is mainly from the nano-antenna due to excitation of LSPs[30,31] (*Supplementary information* **Fig. S4**).

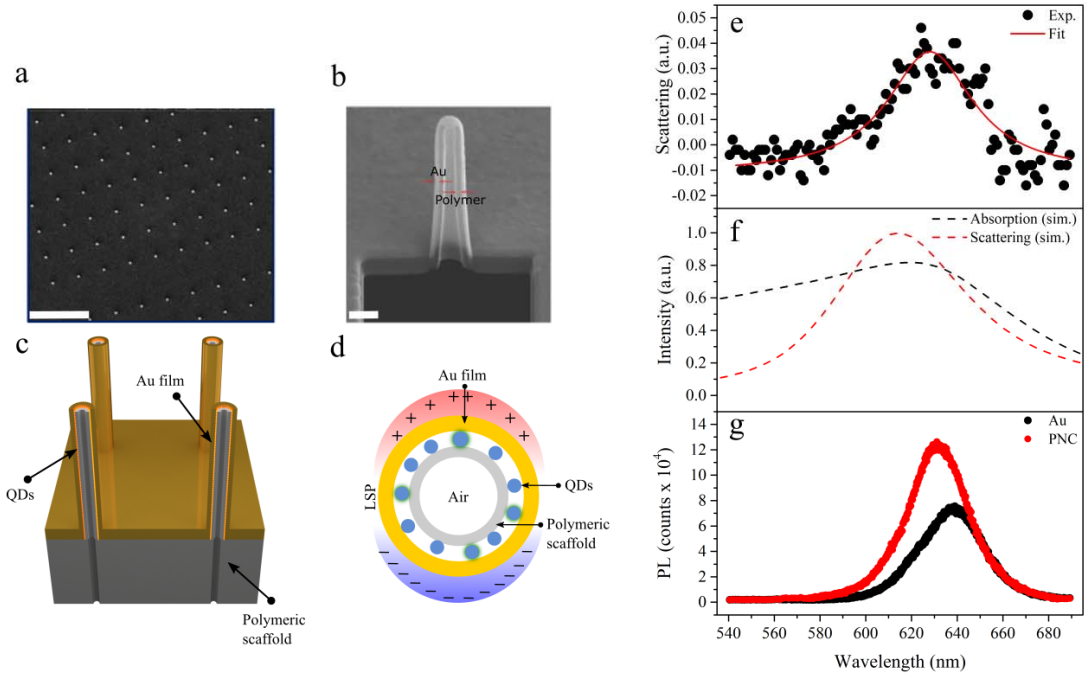

Figure 2| (a) SEM image of plasmonic nanocavity (PNC) array (scale bar= 5 µm). **(b)** SEM image of a cross-section of a single PNC that was cut using focused ion beam FIB (scale bar = 100 nm). **(c)** Schematic of the nano-pillar PNC. The quantum dots (QDs) are spin-coated on a polymeric scaffold, then an Au layer is deposited**. (d)** Schematic of a cross-section of a single nanopillar. Incident light excites QDs that, subsequently, transfer their energy to excite localized surface plasmons (LSPs) which decay into a photon. **(e)** Measured scattering for PNC array; the resonance maximum was determined by fitting the data with a Lorentzian function. The measured resonance closely agrees with the calculated absorption and scattering presented in **(f). (g)** Shows the photoluminescence of QDs spin coated on an Au film vs. QDs incorporated in a single PNC.

Figure 3a shows the time-resolved photoluminescence from a single PNC and the reference Au film for different pump intensities (3.7 W/cm^2- 74 W/cm^2) and $490\,nm$ excitation wavelength (*Supplementary Methods*). The reference sample measured lifetime shows no changes upon increasing the excitation intensity. Conversely, the PNC photoluminescence lifetime strongly depends on the excitation intensity. We fitted the photoluminescence decay curves with bi-exponential functions obtaining two characteristic decay times: a fast (slow) SE rate due to a short (long) living state, as shown in **Fig. 3b**. It is known that CdSe/ZnS quantum dots have fast and slow SE rate components (*Supplementary Note* **2.5**, and **Fig. S5**)[32]. By increasing the pump intensity, the SE rates increased linearly up to six-fold for the PNCs, while no changes were measured for the Au film, as shown in **Fig. 3b**. This linear dependence of the SE rate on the excitation intensity, accompanied by linear increase of the photoluminescence, is a clear signature of a plasmon-mediated CET. It is important to note that the QDs in both the PNC and the reference samples are subjected to comparable excitation conditions (*Supplementary information*, **Fig. S6** and **S7)**

The demonstrated dynamic control of QEs' SE rate in real time and at room temperature presents a significant challenge as it requires modifying the LDOS at a rate faster than the QEs SE rate (~ 1GHz). The ability to do so would enables multiplexing in optical communication and modulation of lasers. Recent works dynamically controlled the fluorescence lifetime of QEs at cryogenic temperatures by controlling the radiation field in real time [24] or by modifying the exciton-cavity coupling strength [25]. Instead, CET mechanism provides real-time, room temperature, control over the SE rate through varying the number of QEs participating in CET. **Figure 3c** shows reversible dynamic control over the SE rate by varying the excitation intensity. Regions with white background represent data taken when the excitation intensity decreased

from 37 to 4.4 W. cm^{-2}, whereas light-blue regions represent data taken by increasing the excitation intensity from 4.4 to 37 W. cm^{-2}. This reversible response offers a complete control on the SE rate and establish the basis for a novel class of optical modulators. Note that in the fourth region, the SE rates are slightly lower for all intensities. This is due to QDs bleaching over long exposure times which decreases *N*, hence, the CET rate.

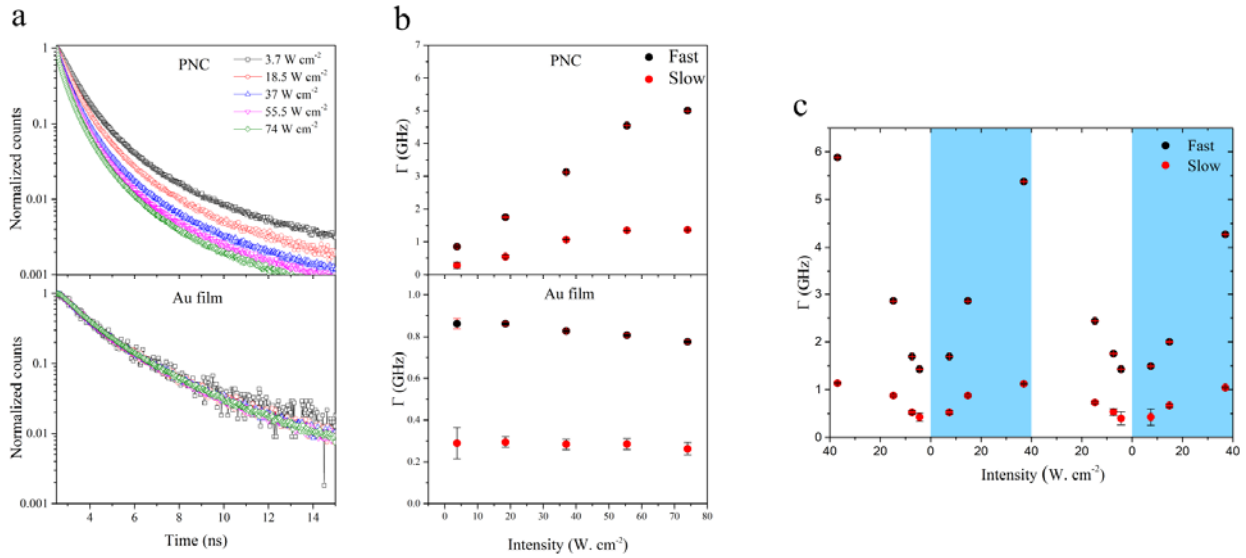

Figure 3| (**a**) Measured time-resolved photoluminescence for five different excitation intensities for the PNC **(Top)** and the reference Au film **(Bottom).** The SE lifetime is intensity dependent only for the PNC. (**b**) The fitted SE rate fast component (black spheres) and slow component (red spheres) for the PNC **(Top)** and for the reference Au film **(Bottom). (c)** Reversible, dynamic control over SE rate. The fast and slow SE rate components vary by modifying *N*. The SE rate is linearly proportional to the excitation intensity.

To quantitatively demonstrate that the linear dependence of the measured SE rate is due to CET, we first investigate the origin of the fast ( ) and slow ( ) SE rates. **Figure 4a** shows the ratio (/ of QDs on the reference Au film as a function of intensity is ~ 3 suggesting that the fast and slow rates correspond to emission of charged biexcitons and charged excitons, respectively, according to the statistical scaling law at room temperature [32]. This is because a charged biexciton (3 electrons and 2 holes) have six decay pathways via electron-hole recombination, while a charged exciton (2 electrons and 1 hole) has only two decay pathways

(**Fig. 4a** inset)- (*Supplementary Note* **2.7**). The SE rate of a QD coupled to a large nano-antenna is $\sim\Gamma^{ET}$. Accordingly, the same statistical scaling applies to energy transfer rates, i.e., $\Gamma_{ET}^{fast}/\Gamma_{ET}^{slow} \sim 3$. Below the saturation intensity, the number of excited QDs participating in CET scales linearly with the excitation intensity I with a scaling factor α, i.e., $N = \alpha I$ (since excited QDs' number is an integer, N here is understood as its average over a small intensity range). The experimentally measured SE rate $\Gamma^{Exp}(I)$ below saturation for QDs participating in CET is given by

$$\Gamma^{Exp}(I) = \Gamma^{ET} + \alpha\,\Gamma^{ET}\,I \qquad (1)$$

where the second term represents the cooperative energy transfer rate in the CET intensity range. For weak excitation intensities, i.e., few emitters are excited, cooperative effects are weak and the experimentally measured SE rate Γ^{Exp} should equal individual QD energy transfer rate Γ^{ET}. Equation (1) holds for both fast and slow rates. Accordingly, the ratio of the experimentally measured Γ^{fast} and Γ^{slow} rates from the PNC is

$$\Gamma^{fast}(I)/\Gamma^{slow}(I) = (\Gamma_{ET}^{fast} + \alpha_{fast}\,\Gamma_{ET}^{fast}\,I)/\,(\Gamma_{ET}^{slow} + \alpha_{slow}\,\Gamma_{ET}^{slow}\,I) \qquad (2)$$

where α_{fast} and α_{slow} are the intensity scaling factors for fast and slow energy transfer rate, respectively. The rates ratio $\Gamma^{fast}(I)/\Gamma^{slow}(I)$ for different intensities is ~3 (**Fig. 4a**), which can only be true if $\alpha_{fast} \approx \alpha_{slow} \approx \alpha$. Since we have two equations and one unknown, α, we can quantitatively validate our analysis using the measured slow rate $\Gamma^{slow}(I) = \Gamma_{ET}^{slow} + \alpha\,\Gamma_{ET}^{slow}\,I$, to calculate α to reproduce the experimentally measured fast rate $\Gamma^{fast} = \Gamma_{ET}^{fast} + +\alpha\ \Gamma_{ET}^{fast}\,I$. **Figure 4b** shows the close agreement between calculated vs. measured Γ^{fast}, indicating that the slope of SE rate intensity dependence is proportional Γ_{ET}^{fast}, as predicted by the CET mechanism.

For relatively higher intensities, the rate ratio exceeds 3 likely because excitons saturate at lower intensities compared to biexcitons [33]. The analysis presented in **Fig. 4a** and **Fig. 4b** for a different PNC is shown in (*Supplementary information,* **Fig. S8**) to confirm our observation reproducibility.

Figure 4c shows the photoluminescence from a PNC vs. excitation intensity. The photoluminescence spectrum retains the plasmon resonance central frequency and overall line-shape while its amplitude increases linearly with excitation power implying that radiation emanates from the PNC following CET [17]. This is in contrast to super-radiance where radiation emanates directly from QEs and changes in the decay rates affect the emission spectra [21]. Furthermore, we exclude stimulated emission and photothermal effects as a cause of SE rate intensity dependence (*Supplementary information*, **Fig. S9**).

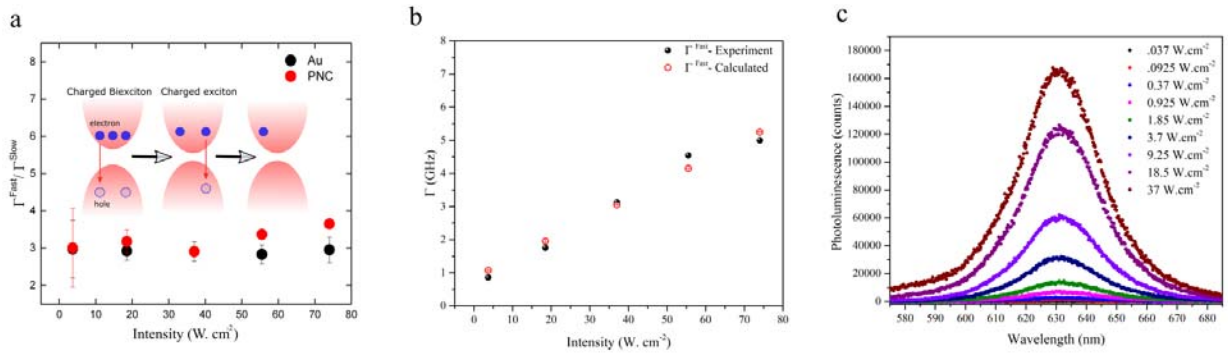

Figure 4| (a) The ratio of the measured fast and slow SE rates for QDs on the reference Au film and inside the PNC. The ratio is ~ 3. Inset: schematic of the decay process of charged biexcitons and charged excitons. **(b)** The rate is calculated from experimental rate by assuming that the slope of the SE rate vs. intensity curve is proportional to the energy transfer rate of individual QD, as predicted by equation (2). (c) The photoluminescence as a function of excitation intensity show that the emission spectrum retains the plasmon lineshape as the peak emission wavelength is ~ 631 nm.

CET represent an additional degree of freedom to control SE beyond the plasmon-enhanced local field [7]. We used a low Q antenna to ensure that the collected photoluminescence is from the PNC. Future works can use high Q and low V nano-antennas [4], to enhance the SE rate beyond

stimulated emission rate (> 100 GHz) which would enable high-speed short-distance optical communication, and enhancing light sources efficiency [6,34,35] (*Supplementary information* **Fig. S10**). Accelerating QDs SE rate can increase the QDs quantum yield by overcoming Auger recombination[36,37]. The demonstrated SE rate-based optical modulator, after overcoming the photobleaching problem, can be used as a multiplexing technique to encode information in the emission rate (*Supplementary Note* **2.12**).

References:

[1] Lodahl P, Floris van Driel A, Nikolaev IS, Irman A, Overgaag K, Vanmaekelbergh D, and Vos WL,Controlling the dynamics of spontaneous emission from quantum dots by photonic crystals.Nature 430, 654 (2004).

[2] Pelton M,Modified spontaneous emission in nanophotonic structures.Nature Photonics 9, 427 (2015).

[3] Purcell EM, Torrey HC, and Pound RV,Resonance Absorption by Nuclear Magnetic Moments in a Solid.Physical Review 69 (1-2), 37 (1946).

[4] Akselrod GM, Argyropoulos C, Hoang TB, Ciracì C, Fang C, Huang J, Smith DR, and Mikkelsen MH,Probing the mechanisms of large Purcell enhancement in plasmonic nanoantennas.Nature Photonics 8, 835 (2014).

[5] El Kabbash M, Rahimi Rashed A, Sreekanth KV, De Luca A, Infusino M, and Strangi G,Plasmon-Exciton Resonant Energy Transfer: Across Scales Hybrid Systems %J Journal of Nanomaterials.Journal of Nanomaterials 2016, 21, 4819040 (2016).

[6] Eggleston MS, Messer K, Zhang L, Yablonovitch E, and Wu MC,Optical antenna enhanced spontaneous emission.Proceedings of the National Academy of Sciences 112 (6), 1704 (2015).

[7] Ciracì C, Hill RT, Mock JJ, Urzhumov Y, Fernández-Domínguez AI, Maier SA, Pendry JB, Chilkoti A, and Smith DR,Probing the Ultimate Limits of Plasmonic Enhancement 337 (6098), 1072 (2012).

[8] Mortensen NA, Raza S, Wubs M, Søndergaard T, and Bozhevolnyi SI,A generalized non-local optical response theory for plasmonic nanostructures.Nature Communications 5, 3809 (2014).

[9] Choquette JJ, Marzlin K-P, and Sanders BC,Superradiance, subradiance, and suppressed superradiance of dipoles near a metal interface.Physical Review A 82 (2), 023827 (2010).

[10] Huidobro PA, Nikitin AY, González-Ballestero C, Martín-Moreno L, and García-Vidal FJ,Superradiance mediated by graphene surface plasmons.Physical Review B 85 (15), 155438 (2012).

[11] Martín-Cano D, Martín-Moreno L, García-Vidal FJ, and Moreno E,Resonance Energy Transfer and Superradiance Mediated by Plasmonic Nanowaveguides.Nano Letters 10 (8), 3129 (2010).

[12] Pustovit VN and Shahbazyan TV,Cooperative emission of light by an ensemble of dipoles near a metal nanoparticle: The plasmonic Dicke effect.Physical Review Letters 102 (7), 077401 (2009).

[13] Pustovit VN and Shahbazyan TV,Plasmon-mediated superradiance near metal nanostructures.Physical Review B 82 (7), 075429 (2010).

[14] Bonifacio R and Lugiato LA,Cooperative radiation processes in two-level systems: Superfluorescence.Physical Review A 11 (5), 1507 (1975).

[15] Cong K, Zhang Q, Wang Y, Noe GT, Belyanin A, and Kono J,Dicke superradiance in solids [Invited].J. Opt. Soc. Am. B 33 (7), C80 (2016).
[16] Shestakov MV, Fron E, Chibotaru LF, and Moshchalkov VV,Plasmonic Dicke Effect in Ag-Nanoclusters-Doped Oxyfluoride Glasses.The Journal of Physical Chemistry C 119 (34), 20051 (2015).
[17] Shahbazyan TV,Cooperative emission mediated by cooperative energy transfer to a plasmonic antenna.Physical Review B 99 (12), 125143 (2019).
[18] Shahbazyan TV,Local Density of States for Nanoplasmonics.Physical Review Letters 117 (20), 207401 (2016).
[19] Novotny L and Hecht B, *Principles of Nano-Optics* (Cambridge University Press, Cambridge, 2006).
[20] Friedberg R, Hartmann SR, and Manassah JT,Frequency shifts in emission and absorption by resonant systems ot two-level atoms.Physics Reports 7 (3), 101 (1973).
[21] Gross M and Haroche S,Superradiance: An essay on the theory of collective spontaneous emission.Physics Reports 93 (5), 301 (1982).
[22] Dicke RH,Coherence in Spontaneous Radiation Processes.Physical Review 93 (1), 99 (1954).
[23] Scheibner M, Schmidt T, Worschech L, Forchel A, Bacher G, Passow T, and Hommel D,Superradiance of quantum dots.Nature Physics 3, 106 (2007).
[24] Jin C-Y, Johne R, Swinkels MY, Hoang TB, Midolo L, van Veldhoven PJ, and Fiore A,Ultrafast non-local control of spontaneous emission.Nature Nanotechnology 9, 886 (2014).
[25] Pagliano F, Cho Y, Xia T, van Otten F, Johne R, and Fiore A,Dynamically controlling the emission of single excitons in photonic crystal cavities.Nature Communications 5, 5786 (2014).
[26] Ryan C *et al.*,Roll-to-Roll Fabrication of Multilayer Films for High Capacity Optical Data Storage.Advanced Materials 24 (38), 5222 (2012).
[27] De Angelis F, Malerba M, Patrini M, Miele E, Das G, Toma A, Zaccaria RP, and Di Fabrizio E,3D Hollow Nanostructures as Building Blocks for Multifunctional Plasmonics.Nano Letters 13 (8), 3553 (2013).
[28] Malerba M *et al.*,3D vertical nanostructures for enhanced infrared plasmonics.Scientific Reports 5, 16436 (2015).
[29] See Supplementary materials for further details https://journals.aps.org/prl/abstract/10.1103/PhysRevLett.122.15791, which includes Refs. [38-43].
[30] Bryant MPGW, *Introduction to metal-nanoparticle plasmonics* (Wiley, 2013), A Wiley-Science Wise Co-Publication.
[31] Ringler M, Schwemer A, Wunderlich M, Nichtl A, Kürzinger K, Klar TA, and Feldmann J,Shaping Emission Spectra of Fluorescent Molecules with Single Plasmonic Nanoresonators.Physical Review Letters 100 (20), 203002 (2008).
[32] Hiroshige N, Ihara T, and Kanemitsu Y,Simultaneously measured photoluminescence lifetime and quantum yield of two-photon cascade emission on single CdSe/ZnS nanocrystals.Physical Review B 95 (24), 245307 (2017).
[33] Matsuzaki K *et al.*,Strong plasmonic enhancement of biexciton emission: controlled coupling of a single quantum dot to a gold nanocone antenna.Scientific Reports 7, 42307 (2017).
[34] Biteen JS, Pacifici D, Lewis NS, and Atwater HA,Enhanced Radiative Emission Rate and Quantum Efficiency in Coupled Silicon Nanocrystal-Nanostructured Gold Emitters.Nano Letters 5 (9), 1768 (2005).
[35] Tsakmakidis K,In the limelight.Nature Materials 11, 1000 (2012).
[36] Gupta S and Waks E,Overcoming Auger recombination in nanocrystal quantum dot laser using spontaneous emission enhancement.Opt. Express 22 (3), 3013 (2014).
[37] Hoang TB, Akselrod GM, Argyropoulos C, Huang J, Smith DR, and Mikkelsen MH,Ultrafast spontaneous emission source using plasmonic nanoantennas.Nature Communications 6, 7788 (2015).
[38] Wang T, Yelin SF, Côté R, Eyler EE, Farooqi SM, Gould PL, Koštrun M, Tong D, and Vrinceanu D,Superradiance in ultracold Rydberg gases. Physical Review A 75 (3), 033802 (2007).

[39] Lippens PE and Lannoo M,Comparison between calculated and experimental values of the lowest excited electronic state of small CdSe crystallites. Physical Review B 41 (9), 6079 (1990).

[40] Young MA, Dieringer JA, and Van Duyne RP, in Tip Enhancement, edited by S. Kawata, and V. M. Shalaev (Elsevier, Amsterdam, 2007), pp. 1.

[41] Khurgin JB,How to deal with the loss in plasmonics and metamaterials. Nature Nanotechnology 10, 2 (2015).

[42] Cueff S, Li D, Zhou Y, Wong FJ, Kurvits JA, Ramanathan S, and Zia R, Dynamic control of light emission faster than the lifetime limit using VO2 phase-change.Nature Communications 6, 8636 (2015).

[43] Lu Y-J, Sokhoyan R, Cheng W-H, Kafaie Shirmanesh G, Davoyan AR, Pala RA, Thyagarajan K, and Atwater HA, Dynamically controlled Purcell enhancement of visible spontaneous emission in a gated plasmonic heterostructure. Nature Communications 8 (1), 1631 (2017).

Acknowledgments: The authors would like to thank Eugenio Calandrini for his help with sample preparation. **Funding:** G.S. received funding from the Ohio Third Frontier Project 'Research Cluster on Surfaces in Advanced Materials (RC-SAM) at Case Western Reserve University' and the GU Malignancies Program of the Case Comprehensive Cancer Center. FDA received funding from the European Research Council under the European Union's Seventh Framework Programme (FP/2007-2013)/ERC Grant Agreement no. [616213], CoG: Neuro-Plasmonics. J.B. received support from U.S. Department of Energy, Office of Science, Basic Energy Sciences, under Award #DE- SC008148. T.V.S was supported in part by NSF grants No. DMR-1610427 and No. HRD-1547754.

Author contributions M.E., T.V.S and G. S. conceived the idea. F.D.A. and E.M. designed and fabricated the samples. M.E., J.B. and G.S. designed the experiments. M.E., A.F., M.W. and E.H. performed experiments. A.B. and M.E. performed simulations. M.E. wrote the manuscript with inputs from all the authors. T.V.S., J.B., F.D.A., and G.S. supervised the research. All authors analyzed and discussed the data.